Exogenous chromosomes reveal how sequence composition drives chromatin assembly, activity, folding and compartmentalization

Christophe Chapard, Léa Meneu, Jacques Serizay, Alex Westbrook, Etienne Routhier, Myriam Ruault, Amaury Bignaud, Agnès Thierry, Géraldine Gourgues, Carole Lartigue, et al.

Exogenous chromosomes reveal how sequence composition drives chromatin assembly, activity, folding and compartmentalization

Christophe Chapard[1,Ψ], Léa Meneu[1,2,Ψ], Jacques Serizay[1,Ψ,*], Alex Westbrook[2,3], Etienne Routhier[2,3,4], Myriam Ruault[5], Amaury Bignaud[1,2], Agnès Thierry[1], Géraldine Gourgues[6], Carole Lartigue[6], Aurèle Piazza[1,#], Angela Taddei[5], Frédéric Beckouët[7], Julien Mozziconacci[3,4,*] and Romain Koszul[1,*]

Affiliation

[1] Institut Pasteur, CNRS UMR 3525, Université Paris Cité, Unité Régulation Spatiale des Génomes, 75015 Paris, France

[2] Sorbonne Université, College Doctoral

[3] Laboratoire Structure et Instabilité des génomes UMR 7196, Muséum National d'Histoire Naturelle, Paris 75005, France

[4] Laboratoire de Physique Théorique des Liquides, Sorbonne Université, CNRS, 75005 Paris, France

[5] Institut Curie, PSL University, Sorbonne Université, CNRS, Nuclear Dynamics, 75005 Paris, France

[6] Univ. Bordeaux, INRAE, Biologie du Fruit et Pathologie, UMR 1332, F-33140 Villenave d'Ornon, France

[7] Molecular, Cellular and Developmental biology department (MCD), Centre de Biologie Intégrative (CBI), Université de Toulouse, CNRS, UPS, 31062, Toulouse, France

[#] Present address: Univ Lyon, ENS, UCBL, CNRS, INSERM, Laboratory of Biology and Modelling of the Cell, UMR5239, U 1210, F-69364, Lyon, France

Ψ These authors contributed equally

* Corresponding authors: romain.koszul@pasteur.fr, julien.mozziconacci@mnhn.fr, jacques.serizay@pasteur.fr

Abstract

Genomic sequences co-evolve with DNA-associated proteins to ensure the multiscale folding of long DNA molecules into functional chromosomes. In eukaryotes, different molecular complexes organize the chromosome's hierarchical structure, ranging from nucleosomes and cohesin-mediated DNA loops to large scale chromatin compartments. To explore the relationships between the DNA sequence composition and the spontaneous loading and activity of these DNA-associated complexes in the absence of co-evolution, we characterized chromatin assembly and activity in yeast strains carrying exogenous bacterial chromosomes that diverged from eukaryotic sequences over 1.5 billion years ago. We show that nucleosome assembly, transcriptional activity, cohesin-mediated looping, and chromatin compartmentalization can occur in a bacterial chromosome with a largely divergent sequence integrated in a eukaryotic host, and that the chromatinization of bacterial chromosomes is highly correlated with their sequence composition. These results are a step forward in understanding how foreign sequences are interpreted by a host nuclear machinery during natural horizontal gene transfers, as well as in synthetic genomics projects.

Introduction

Genome sequence composition, broadly defined by its GC%, polynucleotide frequencies, DNA motifs and repeats, varies widely between species as well as within individual genomes[1,2]. In eukaryotes, the sequence composition is known to correlate with: 1) chromatin composition, which includes nucleosome formation and binding of structural and functional proteins to DNA [3], 2) chromatin activity, such as transcription and replication [4], and 3) functional 3D organization of the genome into loops and compartments [5,6]. For instance in mammals GC-rich regions are enriched in actively transcribed sequences and in chromatin loops mediated by the structural maintenance of chromosomes (SMC) cohesin, and genomic loci with different sequence composition tend to coalesce in distinct compartments [7]. These relationships between sequence and chromatin composition activities and folding reflect their continuous coevolution over millions of years.

Disruptive variations in sequence composition can also emerge naturally during evolution, e.g. through transfer of genetic material across species by horizontal gene transfers or introgression, in viral infections [8–11], or even artificially, e.g. by introducing chromosome-long DNA molecules into chassis microbial strains or cell lines [12–14]. Such transfer can lead to the long-term integration of foreign DNA whose sequence composition strongly diverges from their host's genome (e.g. the introgression of a 12% GC-divergent 1Mb sequence in *Lachancea kluyveri* [15]). Once integrated, these sequences are organized and processed by chromatin-associated proteins of the host genome, obeying new rules under which they have not coevolved. How a eukaryotic host can successfully package, fold and regulate the activity of chromosome-long exogenous bacterial DNA sequences, and the importance of the sequence composition, remain largely unknown. Addressing this question would improve our understanding of the evolutionary processes and sequence determinants involved in chromatin folding and activity.

Here we explored whether and how foreign bacterial full-length chromosomes acquire chromatin features when integrated in a eukaryotic nucleus, and the relationship between their sequence composition and their chromatinization. To this end, we investigated the behavior of two individual bacterial chromosomes with different sequence composition, artificially introduced into the *S. cerevisiae* genome [16,17]. We profiled nucleosome assembly, polymerase and cohesin binding and activities, as well as the 3D chromosome organization during the cell cycle. We show that bacterial chromosomes with different sequence composition present different profiles of chromatin composition and activities, eventually leading to the spontaneous formation of active / inactive chromosomal compartments, similar to the ones observed in complex multicellular organisms. Using neural networks (NNs), we further show that eukaryotic sequence determinants are sufficient to predict the chromatin composition and activity of exogenous chromosomes integrated in the yeast genome. Consequently, this study suggests that the fate of any DNA molecule introduced into a given cellular context, including its organization from nucleosome positioning up to 3D folding and transcriptional activity, is governed by rules that are both deterministic and predictable.

Results

Adaptation of supernumerary bacteria chromosomes to yeast

To investigate large sequences which have not evolved in a eukaryotic context, we exploited *S. cerevisiae* strains carrying an extra 17th circular chromosome made either from the *Mycoplasma mycoides* subsp. *mycoides* (referred to as “Mmyco”) or *Mycoplasma pneumoniae* (“Mpneumo”) genomes containing a yeast centromeric sequence and an autonomous replication sequence (ARS) [18] (**Methods**; **Table S1**). While the GC content of *S. cerevisiae* is 38%, the GC content of the Mmyco and Mpneumo chromosomes 24% (GC-poor) and 40% (GC-neutral), respectively (**Fig. 1a**). Dinucleotide composition, estimated by the dinucleotide odds

ratio ρ*(XY) [19], also largely differs between yeast and bacterial chromosomes (**Extended Data Fig. 1a**).

We linearized these chromosomes, added yeast telomeres at the extremities (**Fig. 1a; Extended Data Fig. 1b**; **Methods**), and investigated their replication and cohesion using split-dot assay and marker frequency analysis (**Extended Data Fig. 1c,d** and **Supplementary Results**; **Methods**). Overall, these chromosomes do not impose a significant fitness cost on their eukaryotic host, with each strain displaying similar growth rates compared to their parental strains in selective media (**Extended Data Fig. 1e**). They also have an estimated segregation rate similar to a centromeric plasmid [20] (**Extended Data Fig. 1f**).

Spontaneous chromatinization of bacterial chromosomes in a eukaryotic context

We first assessed whether integrated Mmyco and Mpneumo chromosomes were able to chromatinize by performing MNase-seq and H3 and H2A ChIP-seq experiments (Methods; **Fig. 1b, c; Extended Data Fig. 2a**). Strikingly, both bacterial chromosomes were able to form nucleosomes and local nucleosome-depleted regions (NDR; **Fig. 1b, c; Extended Data Fig. 2b-d**). Nucleosomes over the Mpneumo chromosome have structural features comparable to yeast nucleosomes, with a linker DNA of ~14 bp and a nucleosomal repeat length (NRL) of 160 bp (**Fig. 1d,e**). In contrast, nucleosomes in the Mmyco chromosome have a longer linker DNA and thus are more spaced than in yeast or Mpneumo chromosomes, with an NRL of 177 bp (**Fig. 1d,e)**. Two sequence features may explain this: first, poly(dA) and poly(dT) tracks, known to promote NDR formation, are over-represented along the Mmyco genome. Secondly, the AA/TT 10-bp periodicity, which facilitates DNA bending around histone cores, is reduced (**Extended Data Fig. 2e,f**). The analysis of MNase-seq time course experiments also revealed that Mmmyco nucleosomal fragments are more rapidly degraded by MNase than yeast or Mpneumo nucleosomal fragments (**Extended Data Fig. 2c,d**), reflecting either the “fragile” nature of AT-rich nucleosomes or the MNAse bias for these sequences [21,22].

We further profiled the chromatin composition of Mmyco and Mpneumo chromosomes by performing RNA polymerase II (PolII) and cohesin (Scc1) ChIP-seq experiments (**Fig. 1f, Extended Data Fig. 2g-j)**. We found that the Scc1 and PolII binding profiles along the Mpneumo chromosome appear similar to wild-type (WT) yeast chromosomes, with discrete Scc1 peaks (**Fig. 1f, Extended Data Fig. 2h,i**) preferentially located in nucleosome-depleted and PolII-enriched regions (**Extended Data Fig. 2j**). In contrast, Scc1 and PolII binding profiles in the Mmyco strain show significant differences. On the one hand, Scc1 is strongly enriched over the whole Mmyco chromosome, but does not form the distinct peaks observed on endogenous chromosomes (**Fig. 1f, Extended Data Fig. 2h,i**). Interestingly, Scc1 levels also appear strongly reduced at centromeres of endogenous *S. cerevisiae* chromosomes (**Extended Data Fig. 2g**), suggesting that the Mmyco chromosome titrates cohesins enriched over yeast centromeres. On the other hand, the PolII profile is greatly reduced along the Mmyco chromosome, compared with yeast chromosomes.

These results show that large exogenous bacterial chromosomes placed in a eukaryotic context spontaneously adopt eukaryotic chromatin composition features: histones, Pol II and cohesins all bind bacterial DNA irrespectively of their sequence composition. However, striking differences in the chromatin profiles led us to define two chromatin types: (1) “Y” (yeast-like) chromatin landscape, found over Mpneumo (whose 40% GC content is close to the native *S. cerevisiae* GC content), and (2) “U” (for Unconventional) chromatin, found over Mmyco (with a low 24% GC content), featuring less packed nucleosomes, a reduced Pol II enrichment, and a broad binding of cohesins across the entire chromosome.

Finally, we find that a convolutional neural network trained on yeast chromosome sequences was able to predict nucleosome, Scc1 and PolII binding profiles along integrated bacterial chromosomes (**Supplementary Results** and **Extended Data Fig. 3**; **Methods**). This indicates that the complex, underlying eukaryotic sequence determinants are successfully

reused to generate these different chromatin landscapes along integrated bacterial chromosomes.

Transcriptional activity of bacterial genomes in a yeast context

We next explored Y and U chromatin activities by first performing total, stranded RNA-seq (**Fig. 2a,b; Method**). Consistent with PolII ChIP-seq profiles (**Fig. 1f**), we find that the Y chromatin type on Mpneumo is transcribed to levels similar to those of endogenous yeast chromosomes (**Fig. 2a**). However, Mpneumo transcription tracks are significantly longer than yeast genes (4.9kb vs 3.4kb, p-value < 2e-4, two-sided Student's t-test) and do not systematically display clear boundaries (**Fig. 2b**). They also do not preferentially occur over bacterial gene bodies nor seem to initiate at bacterial promoters, also consistent with an absence of PolII enrichment at these loci (**Extended Data Fig. 4a-c**).

In sharp contrast, the Mmyco U chromatin type is only sparsely and lowly transcribed (**Fig. 2a,b**), again in good agreement with the reduced levels of PolII deposition (**Fig. 1f**). This transcriptional inactivity is not associated with the recruitment of the yeast silencing complex SIR Sir2/3/4 [23] (**Extended Data Fig. 4d**).

Intriguingly, the transcription tracks orientation along bacterial chromosomes follows, on average, the orientation of the bacterial genes annotated along these sequences, although the transcription machinery has diverged billions years ago (**Fig. 2c**, see the orientation of genes and stranded tracks in **Fig. 2a,b**). This correlates with the over-representation of A (G) compared to T (C) on the coding strand, both detected in yeast genes and bacterial genes (**Extended Data Fig. 4e**, see **Discussion**).

Inactive U chromatin forms a compartment into the nuclear space in G1

To assess the 3D organization of Y and U chromatin types, we performed capture of chromosome conformation (Hi-C) [24] experiments on the Mmyco or Mpneumo strains arrested either in G1 or G2/M (**Fig. 3a, b**).

In G1-arrested cells, yeast chromosomes exhibit the expected Rabl configuration, with clustered centromeres and subtelomeric regions, resulting in a dotted pattern in Hi-C contact maps [25,26]. For both Mmyco and Mpneumo chromosomes, the added yeast centromeric sequence clusters with the native yeast centromeres. However, the two bacterial chromosomes exhibit very distinct structural characteristics (**Fig. 3a**). The Y-type Mpneumo chromosome behaves as an endogenous *S. cerevisiae* chromosome (**Fig. 3a**), with similar trans-contacts (**Extended Data Fig. 5a**) and long-range cis-contacts (**Fig. 3c**), and a slope of the averaged contact probability (p) as a function of the genomic distance (*s)* close to -1.5, a value corresponding to the typical polymer structure observed in simulations (**Fig. 3c**) [27]. In addition, DNA-FISH labeling of Mpneumo DNA reveals an extended and contorted structure within the intranuclear space, confirming the intermixing of the chromosome with the actively transcribed native chromosomes (**Fig. 3e, Extended Data Fig. 5c,d**).

In contrast, in the U-type Mmyco chromosome, (1) only few contacts were detected with the endogenous chromosomes (**Extended Data Fig. 5a**), and predominantly with the 32 yeast subtelomeric regions (**Fig. 3a**, dotted rectangles; **Extended Data Fig. 5b**); (2) the slope of the p(s) curve also changes dramatically towards a value of -1 at shorter distances, corresponding to a polymer globule (**Fig. 3c**) [24]; (3) DNA-FISH labeling of the Mmyco chromosome confirmed the globular conformation of the chromosome and revealed its preferential position at the nuclear periphery, reflecting its proximity with sub/telomeres (**Fig. 3e; Extended Data Fig. 5c,d**). These results show that inactive, U chromatin forms a compartment in the nuclear space segregated from the active endogenous chromosomal set.

Cohesin compacts similarly both exogenous bacterial chromosomes during G2/M

We then generated Hi-C contact maps of both strains synchronized in G2/M. In yeast, chromosome compaction in G2/M-arrested cells reflect cohesin-mediated chromatin folding into arrays of loops, with cohesin peaks corresponding to loop anchors [28,29]. This compaction results in a typical p(s) curve that presents an inflection point around the average loop length [25]. The decrease of interchromosomal contacts (**Fig. 3b, Extended Data Fig. 5a)** and of p(s) (**Fig. 3d, Extended Data Fig. 5e,f**) observed for both native and bacterial chromosomes indicate a similar mitotic compaction of both Y and U chromatin types.

Yeast and Mpneumo chromosomes exhibit focal contact Scc1 enrichments corresponding to cohesin-anchored loops (black triangles on **Fig. 3f**) [28]. We found that cohesin accumulates at sites of convergent transcription not only, as expected, on yeast chromosomes [30,31], but also on Mpneumo (**Fig. 2b**, green dotted lines, **Extended Data Fig. 5g**), with strong cohesin peaks associated with sharper transcriptional convergence (**Fig. 2b**, arrows; **Extended Data Fig. 5h,i**). Using Chromosight, we identified 59 loops across the Mpneumo chromosome, spanning over slightly longer genomic distances (28 kb on average) than the loops found along yeast sequences (22 kb) (**Extended Data Fig. 5j**; **Methods**), and with strong Scc1 peaks positioned close to anchors, with a median distance of 566 bp (**Fig. 3f, h**). The dotted grid pattern in Mpneumo is reminiscent of multiple DNA loops observed along mammalian interphase chromosomes [32], suggesting that some loop anchors have the ability to be involved in loops of various sizes, a phenomenon not observed across native *S. cerevisiae* chromosomes (**Fig. 3f**).

On the other hand, no visible discrete loops were observed along the Mmyco chromosome where cohesins cover inactive U chromatin regions without clear peaks, probably reflecting the absence of (convergent) transcription (**Fig. 3g**) (**Fig. 1f** and **Fig. 2b**). These results suggest that cohesin can bind DNA and promote compaction in absence of active transcription, but doest accumulate at discrete positions.

Cohesin-mediated loops along yeast chromosomes are formed through loop extrusion (LE), a process by which cohesin complexes organize DNA by capturing and gradually enlarging

small loops [33,34]. To test whether LE compacts bacterial genomes, we performed Hi-C in absence of Wpl1 (human Wapl), which impairs cohesin removal and results in longer loops readily visible by a shift of the inflection point in the p(s) curve [28,34]. In absence of Wpl1, we observed increased long-range contacts in all chromosomes, including Mmyco and Mpneumo (**Fig. 3i; Extended Data Fig. 5k**), consistent with active cohesin-mediated LE proceeding on both Y and U chromatin.

Overall, these observations highlight two different spatial configurations of Mmyco and Mpneumo exogenous chromosomes. On the one hand, the inactive Mmyco chromosome in G1 is compacted and positioned at the periphery of the nucleus, away from the active chromosome set. Upon S-phase and G2 arrest, the DNA is nevertheless compacted in a cohesin-dependent manner with no visible loops at discrete positions. On the other hand, the active Mpneumo chromosome behaves as endogenous yeast chromosomes, displaying discrete mitotic DNA loops in G2/M.

Mosaic chimeric chromosomes display spontaneous, chromatin type-dependent DNA compartmentalization

The structural and functional features of the Y- and U-type chromatin are reminiscent of the euchromatin and heterochromatin compartments described along metazoan chromosomes [24]. We wondered whether they can coexist on a single chromosome. Using CRISPR-Cas9, we first fused the Mmyco chromosome with the native yeast chromosome XVI (XVIfMmyco chromosome). We then induced translocations to generate two other strains with chromosomes harboring alternating U and Y chromatin regions as small as 50 kb (XVIfMmycot1 and XVIfMmycot2; **Fig. 4a**; **Extended Data Fig. 6a-c** Methods). ChIP-seq profiles of RNA PolII on Mmyco regions were similar before and after translocation, demonstrating that PolII binding is independent of the broader regional context (**Extended Data Fig. 6d**). The overall Hi-C contact maps of XVIfMmyco strain synchronized in G1 showed little differences compared to the

parental Mmyco strain (but for the deleted and fused regions) (**Fig. 4b**, compare panel **i** with **ii**). The Y-type chr. XVI arm intermixes with the other 15 yeast chromosomes while the U-type Mmyco arm remains isolated from the rest of the genome, contacting subtelomeric regions (**Fig. 4b**). In the translocated strains, however, the alternating chromatin type regions resulted in striking checkerboard contact patterns within XVIfMmycot1 and XVIfMmycot2 chromosomes (**Fig. 4b**, panels **iii** and **iv**). This pattern reflects the fact that U-type regions make specific contacts over long distances, bypassing the Y-type regions found in between (**Fig. 4c**; **Extended Data Fig. 6e** G1). Similarly, Y-type regions of chromosome XVI also are also involved in specific Y-Y contacts over longer distances (**Fig. 4c**). Intra U and Y regions contact decay is also different in the two chromatin types, U chromatin being prone to longer range contacts in cis (**Extended Data Fig. 6e**). We then induced another translocation to integrate a segment of U chromatin in a *trans* position at the end of chromosome XIII and generated the corresponding Hi-C map (**Fig. 4d**). The correlation and 4C-like plot revealed an increase in inter-chromosomal contacts between Y chromatin segments with distant segments of itself, and in alternance with decreased contacts with Mmyco U chromatin segments (and vice versa), showing that the inactive U chromatin compartment can contain segments positioned on different chromosomes (**Fig. 4d**). These results unambiguously show that in yeast alternated or inter-chromosomal segments of active and inactive chromatin are spontaneously segregated within the nuclear space in G1 (**Fig. 4e, Extended Data Fig. 6h)**, a phenomenon reminiscent of eu- and heterochromatin compartments found in higher eukaryotes [24].

In G2/M, the Scc1 deposition pattern, including centromere depletion, remained conserved along mosaic chromosomes (**Extended Data Fig. 6d**). Cohesin coating remained enriched over U-type Mmyco sequences, including over the 50 kb encompassed within 850 Mb of yeast DNA on XVIfMmycot2 chromosome. These results show that cohesin is loaded along inactive Mmyco regions independently of the proximity with the centromere (as along WT chromosomes) and

244 independently of transcription, suggesting that the larger chromatin context plays little role in
245 cohesin-mediated loading. In addition, Hi-C maps of the mosaic chromosomes in G2/M show
246 that U-type compartments disappear upon cohesin-mediated compaction (**Extended Data Fig.**
247 **6f**). The analysis of distance-dependent contact frequency shows that all chromosome regions
248 behave similarly at this stage (**Extended Data Fig. 6e**, G2/M). The only noticeable difference
249 resulting from the fusion/translocation events in G2/M Hi-C contact maps consists in a DNA loop
250 appearing over the boundary between Mmyco and the endogenous yeast sequence (**Extended**
251 **Data Fig. 6f,g**). The two anchors of the loop are a strongly cohesin-enriched region already
252 present on chr. XVI sequence, and another region slightly enriched in cohesin already present
253 on the Mmyco sequence (**Extended Data Fig. 6g**, green arrows).

254 Together with observations from the previous section, these results show that Y and U
255 chromatin types are both prone to dynamic cohesin-dependent DNA compaction and loop
256 formation in G2/M phase (**Fig. 4e**) and further suggest that loop extrusion can proceed through
257 the Y/U chromatin junction to form a loop bridging the nearest cohesin enrichment sites on each
258 side [35,36]. Therefore, as observed in multicellular organisms, LE-mediated metaphase
259 chromosome compaction abolishes chromatin compartments to prepare chromosomes for
260 segregation (**Fig. 4e)** [33,37].
261

262 ## Discussion

263 *Chromatin composition and activity of bacterial DNA follows yeast sequence determinants*
264 Several studies have shown that exogenous or random DNA segments in the yeast nucleus
265 with a GC% relatively similar to that of yeast chromosome are actively transcribed [38–41]. Here we
266 explore the relationships between sequence composition and chromatin composition and
267 activity by characterizing large, divergent bacterial DNA sequences in a eukaryotic cellular
268 context into which they have not evolved. We find that *M. pneumoniae* and *M. mycoides*

chromosomes integrated in yeast adopt one of two archetypes of chromatin that we called Y and U for yeast-like and unconventional. In both types, nucleosomes can assemble albeit with a longer NRL in the U chromatin (177 vs 160 bp), which also correlates with a low transcription. In G1, transcriptionally inactive U chromatin segments spontaneously collapse into a globule leading to the formation of a new nuclear compartment, whereas Y chromatin intermixes with yeast endogenous DNA. In G2/M, SMC cohesin complexes bind to both chromatin types and compact DNA through the extrusion of DNA loops [6]. Along Y chromatin, these complexes accumulate at convergent transcription loci [28,30], whereas along U chromatin, the absence of active transcription leads to a homogeneous enrichment pattern.

The chromatin composition and activity experimentally measured over these exogenous chromosomes can be predicted using convolutional neural networks solely trained on yeast sequences, showing that exogenous DNA composition obeys a set of host rules based on sequence determinants that include GC content, dinucleotide composition but also complex sequence features. Sequence composition is therefore an important driver of the chromatin composition of exogenous sequences.

Prokaryotic DNA contains some determinants of transcription orientation in eukaryote

Active transcription on bacterial chromosomes in yeast follows, on average, bacteria genes orientation (**Fig. 2**). Several mechanisms could account for this observation. Sequence determinants predating the divergence of eucaryotes and procaryotes, including GC and AT skews, are known to influence polymerase directionality [47,48]. Alternatively, bacteria codon usage bias could result in enrichment in Nrd1-Nab3-Sen1 (NNS) binding sites along the ncRNA strand, leading to transcription termination [39,49]. The Nonsense-Mediated Decay (NMD) complex, which destabilizes in the cytoplasm eukaryotic transcripts with long 3' UTR, could also be more frequently activated by bacteria RNA transcribed in an antisense orientation. Eventually, the resulting conserved orientation could facilitate the domestication of exogenous

295 sequences during horizontal transfer/introgression events between distant species. Whether
296 these RNA molecules are translated, and peptides of bacterial origins exist in the yeast cell,
297 remains to be determined. If so, they could provide a source of diversity and adaptation.
298
299 *Cohesin-mediated chromatin folding along non-transcribed DNA templates*
300 It is proposed that cohesins expand DNA loops by an active process of loop extrusion until
301 they encounter an obstacle and/or a release signal [6,33]. For instance, the transcriptional
302 repressor CTCF constitutes a cohesin roadblock to LE in mammals, but SMC-mediated loops
303 have been identified in genomes lacking CTCF across domains of life. In yeast and other
304 species, anchors are thought to be determined by a combination of convergent transcription,
305 replication fork progression during S phase and/or the presence at these positions of stably
306 bound cohesin promoting sister chromatid cohesion [50–52]. The barely transcribed Mmyco
307 chromosome is compacted by cohesin at G2/M, without discrete loop anchoring, suggesting that
308 transcription is neither necessary for loading nor a primary driver for translocation. We propose
309 that cohesins can move freely along this template without encountering significant obstacles,
310 making it a suitable model for studying potentially blocking sequences or molecules.
311
312 *Compartmentalization of foreign DNA in host's nucleus*
313 We show that the introduction a foreign DNA with a lower GC content is sufficient to
314 spontaneously promote the formation of a distinct inactive chromatin type, with increased NRL
315 and a compact globular structure, all features reminiscent of mammalian heterochromatin. This
316 chromatin forms a new compartment at the periphery of the budding yeast nucleus (**Fig. 5e;**
317 **Extended Data Fig. 6h**), like the metazoan compartment "B" formed by inactive,
318 H3K9me3/HP1-mediated heterochromatin, which is absent in yeast. The mechanisms behind
319 compartmentalization remain unknown, but we hypothesize that the unmixing between U and Y
320 chromatin could be due either to NRL change, protein composition and/or activity. Importantly,

longer NRLs are found in heterochromatin in mammals, and are associated with histone H1 [53]. In contrast, Y chromatin intermixes with active yeast DNA.

Depending on its sequence composition, a DNA molecule will therefore either compartmentalize or intermix with the host DNA. These different fates of the two chromatin types raise interesting evolutionary considerations. In the context of the invasion of the genome by exogenous mobile elements, this could lead either to the spontaneous isolation of inactive foreign DNA or, on the contrary, to the co-option of a new set of active sequences that could represent a reservoir of genetic innovations. This sequence-dependent mechanism may have contributed to the heterochromatinization of AT-rich transposable elements integrated in mammalian genomes.

Competing interests

The authors declare no competing interests.

Authors Contributions

Conceptualization: CC, LM, JS, JM and RK. Methodology: LM, CC, JS, CL, JM, RK. Software: JS. Validation: CC, JS, LM. Investigation: LM, CC, with contributions from AP, AB, AgT MR and FB. Formal analysis: JS, AW, ER, CC, LM, FB, MR, AnT. Data Curation: JS, with contributions from CC, LM. Resources: GG, CL. Visualization: JS. Writing - original draft preparation: CC, JS, LM, JM and RK. Writing – Editing: all authors. Writing – Revisions: JS, LM, AW, JM, RK. Supervision: JM, RK. CC co-supervised a student. Funding acquisition: RK. Project Administration: RK.

Acknowledgements

We are grateful to Bernard Dujon, Micheline Fromont-Racine, Alain Jacquier, Gianni Liti, Bertrand Llorente, Marcelo Nollmann, Cosmin Saveanu and Benoit le Tallec for fruitful comments on the work and the manuscript. This research was supported by the European Research Council under the Horizon 2020 Program (ERC grant agreement 771813) and Agence Nationale pour la Recherche (ANR-19-CE13-0027-02) to RK. RK, FB, JM and AnT also received support from Agence Nationale pour la Recherche (ANR-22-CE12-0013-01). CC was supported by a Pasteur-Roux-Cantarini fellowship. JS was supported by a postdoctoral ARC fellowship. We thank all our colleagues from the laboratory régulation spatiale des génomes for fruitful discussions. We especially thank Cyril Matthey-Doret for support during the earlier steps of the project. E. Turc and L. Lemée at Biomics Platform, C2RT, Institut Pasteur, Paris, France, are supported by France Génomique (ANR-10-INBS-09-09) and IBISA for processing and sequencing RNA samples.

Figure legends

Figure 1. Chromatin composition of bacterial chromosomes in yeast.

a, Schematic representation of the conversion from circular to linear chromosomes integrated in yeast. The purple and blue colors represent the *M. pneumoniae* (Mpneumo) and *M. mycoides* (Mmyco) bacterial sequence in all figures, respectively. Right: distribution of GC% for 1kb windows over yeast chromosome XVI, *M. pneumoniae* and *M. mycoides* chromosomes.

b, Nucleosomal track (grey, see **Methods**) and H2A and H3 ChIP-seq (shades of blue, IP vs input, log2) profiles obtained in the Mpneumo strain (*S. cerevisiae* + *M. pneumoniae*). 10kb-long genomic windows from the chromosome XVI (left: 250kb-260kb) and the Mpneumo chromosome (right: 710kb-720kb) are shown at the same scale. Genomic loci highlighted in yellow correspond to nucleosome-depleted regions.

c, Same as **b** in the Mmyco strain (*S. cerevisiae* + *M. mycoides*). 10kb-long genomic windows from chromosome XVI (left: 250kb-260kb) and the Mmyco chromosome (right: 989kb-999kb) are shown at the same scale.

d, Frequency of nucleosome linker DNA length in Mpneumo and Mmyco strains. For each strain, the distribution is calculated for each chromosome separately. The dashed line indicates 14 bp and the dotted line indicates 25 bp.

e, Auto-correlation of the nucleosome track in Mpneumo and Mmyco strains, computed for each chromosome separately (lag <= 1000). Nucleosome repeat length (NRL) is indicated for yeast, Mpneumo and Mmyco chromosomes.

f, Scc1 (red) and RNA Pol II (green) ChIP-seq profiles (IP vs input, log2) obtained in the Mpneumo (left) or in the Mmyco (right) strains. For each strain, 60kb-long genomic windows from the bacterial chromosome and the chromosome XVI are shown, at the same scale. GC% in sliding 1kb windows is shown below the ChIP-seq profiles.

Figure 2. Expression of exogenic bacterial sequences in budding yeast.

a, Stranded RNA-seq profiles along yeast chromosome XVI or along bacterial chromosomes Mpneumo and Mmyco in the corresponding strains. Forward (pink) and reverse (turquoise) genes along yeast or bacterial sequences are indicated as transparent segments under the tracks. Pink and turquoise represent forward and reverse transcription, respectively.

b, Top: stranded RNA-seq profiles along a 60kb window along yeast chromosome XVI, Mpneumo or Mmyco. Bottom: Scc1 (cohesin) deposition profiles of the corresponding loci. Green dotted lines indicate identified loci of convergent transcription (see Methods).

c, Forward and reverse RNA-seq coverage of forward- and reverse-oriented yeast or bacterial genes. Scores were normalized by the length of each genomic feature.

Figure 3. Folding of exogenic bacterial sequences within the yeast nucleus.

a, b, Hi-C contact maps of representative endogenous and of Mmyco and Mpneumo bacterial chromosomes in G1 (**a**) and G2/M (**b**) (4kb resolution).

c, **d**, Contact frequency (p) as a function of genomic distance (s) plots of endogenous yeast chromosomes (long arms) and of Mmyco and Mpneumo bacterial chromosomes in G1 (**c**) and G2/M (**d**).

e, Left: FISH imaging. Representative field of either (top) Mpneumo or (bottom) Mmyco fixed cells labeled with DAPI (left panel) and hybridized with a fluorescent probe generated from either the Mpneumo or Mmyco chromosome, respectively. Right: For each probe, number of patches detected per nucleus and surface occupied by these patches relative to the whole nucleus surface (Methods).

f, g, Top: magnification of 150kb windows from Hi-C contact maps in G2/M from either an endogenous or the bacterial chromosome in Mpneumo (**f**) and Mmyco (**g**) strains (1kb

406 resolution). Bottom: Scc1 ChIP-seq deposition profile. Black arrowheads: loops. Cyan
407 diamonds: Scc1 peaks positions.
408 **h,** Left: distance between chromatin loop anchors and the nearest Scc1 peak in Mpneumo (with
409 and without a random shuffle of peak positions). Right: Scc1 peak strengths in yeast or
410 Mpneumo chromosome, near (< 1kb) or outside loop anchors (p-values from two-sided
411 Student's t-test).
412 **i,** Distance-dependent contact frequency in endogenous yeast and in bacterial chromosomes
413 (left, Mpneumo; right, Mmyco), in WT (dashed) and in Δwpl1 mutants.
414
415 **Figure 4. Compartmentalization of mosaic chromosomes composed of Y and U-type**
416 **chromatin.**
417 **a,** Schematic representation of the CRISPR strategy used to generate the Mmyco mosaic
418 chromosomes with alternating Y and U chromatin regions.
419 **b**, Top: G1 Hi-C contact maps of chr. XV, XVI, and bacterial chromosomes in the Mmyco strain,
420 and in translocated derivatives from panel **a**) (4kb resolution). Bottom: correlation matrices of
421 the corresponding contact maps.
422 **c,** Virtual 4C profiles of viewpoints (grey/blue arrows) located within yeast chr. XVI (in grey) or
423 Mmyco chromosome segments (in blue), in XVIfMmyco (top), XVIfMmycot1 (middle) and
424 XVIfMmycot2 (bottom) strains.
425 **d,** Left: Schematic representation of the CRISPR strategy used to generate the Mmyco mosaic
426 XVIfMmycot3 strain, with alternating yeast and Mmyco segments in chromosomes XIII and XVI.
427 Middle: G1 Hi-C maps of mosaic chromosomes XIII and XVI in XVIfMmycot3 strain. The color
428 scales for the normalized contact map and the correlation matrix are the same as in **b**. Right:
429 Virtual 4C profiles of viewpoints located within yeast chr. XIII (in grey) or within yeast chr. XVI (in
430 grey) or Mmyco chromosome (in blue) segments in XVIfMmycot3 strain. Grey/blue arrows:Y
431 and U chromatin viewpoints position.

e, Schematic of a chimeric chromosome composed of alternating Y- and U-type chromatin. Left: composition of Y- and U-type chromatin. Middle: Spatial and functional organization in G1. Right: Organization of Y and U-type chromatin segments in G2/M.

References

1. Romiguier, J., Ranwez, V., Douzery, E. J. P. & Galtier, N. Contrasting GC-content dynamics across 33 mammalian genomes: relationship with life-history traits and chromosome sizes. *Genome Res* **20**, 1001–1009 (2010).
2. Tajbakhsh, J. *et al.* Spatial Distribution of GC- and AT-Rich DNA Sequences within Human Chromosome Territories. *Experimental Cell Research* **255**, 229–237 (2000).
3. Valouev, A. Determinants of nucleosome organization in primary human cells. *Nature* **474**, 516–520 (2011).
4. Holmquist, G. P. Evolution of chromosome bands: Molecular ecology of noncoding DNA. *J Mol Evol* **28**, 469–486 (1989).
5. Mirny, L. & Dekker, J. Mechanisms of Chromosome Folding and Nuclear Organization: Their Interplay and Open Questions. *Cold Spring Harb Perspect Biol* **14**, a040147 (2022).
6. Davidson, I. F. & Peters, J.-M. Genome folding through loop extrusion by SMC complexes. *Nat Rev Mol Cell Biol* (2021) doi:10.1038/s41580-021-00349-7.
7. Belmont, A. S. Nuclear Compartments: An Incomplete Primer to Nuclear Compartments, Bodies, and Genome Organization Relative to Nuclear Architecture. *Cold Spring Harb Perspect Biol* **14**, a041268 (2022).
8. Crisp, A., Boschetti, C., Perry, M., Tunnacliffe, A. & Micklem, G. Expression of multiple horizontally acquired genes is a hallmark of both vertebrate and invertebrate genomes. *Genome Biol* **16**, 50 (2015).
9. Edelman, N. B. & Mallet, J. Prevalence and Adaptive Impact of Introgression. *Annu Rev Genet* **55**, 265–283 (2021).
10. Van Etten, J. & Bhattacharya, D. Horizontal Gene Transfer in Eukaryotes: Not if, but How Much? *Trends Genet* **36**, 915–925 (2020).

11. Peter, J. *et al.* Genome evolution across 1,011 Saccharomyces cerevisiae isolates. *Nature* **556**, 339–344 (2018).
12. Baby, V. *et al.* Cloning and Transplantation of the Mesoplasma florum Genome. *ACS Synth Biol* **7**, 209–217 (2018).
13. Coradini, A. L. V., Hull, C. B. & Ehrenreich, I. M. Building genomes to understand biology. *Nat Commun* **11**, 6177 (2020).
14. Currin, A. *et al.* The evolving art of creating genetic diversity: From directed evolution to synthetic biology. *Biotechnol Adv* **50**, 107762 (2021).
15. Payen, C. *et al.* Unusual composition of a yeast chromosome arm is associated with its delayed replication. *Genome Res.* **19**, 1710–1721 (2009).
16. Labroussaa, F. *et al.* Impact of donor-recipient phylogenetic distance on bacterial genome transplantation. *Nucleic Acids Res* **44**, 8501–8511 (2016).
17. Ruiz, E. *et al.* CReasPy-Cloning: A Method for Simultaneous Cloning and Engineering of Megabase-Sized Genomes in Yeast Using the CRISPR-Cas9 System. *ACS Synth Biol* **8**, 2547–2557 (2019).
18. Lartigue, C. Creating bacterial strains from genomes that have been cloned and engineered in yeast. *Science* **325**, 1693–1696 (2009).
19. Karlin, S. & Mrázek, J. Compositional differences within and between eukaryotic genomes. *Proceedings of the National Academy of Sciences* **94**, 10227–10232 (1997).
20. Christianson, T. W., Sikorski, R. S., Dante, M., Shero, J. H. & Hieter, P. Multifunctional yeast high-copy-number shuttle vectors. *Gene* **110**, 119–122 (1992).
21. Chereji, R. V., Ocampo, J. & Clark, D. J. MNase-Sensitive Complexes in Yeast: Nucleosomes and Non-histone Barriers. *Mol Cell* **65**, 565-577.e3 (2017).
22. Xi, Y., Yao, J., Chen, R., Li, W. & He, X. Nucleosome fragility reveals novel functional states of chromatin and poises genes for activation. *Genome Res.* **21**, 718–724 (2011).

23. Kueng, S., Oppikofer, M. & Gasser, S. M. SIR proteins and the assembly of silent chromatin in budding yeast. *Annu Rev Genet* **47**, 275–306 (2013).

24. Lieberman-Aiden, E. *et al.* Comprehensive Mapping of Long-Range Interactions Reveals Folding Principles of the Human Genome. *Science* **326**, 289–293 (2009).

25. Lazar-Stefanita, L. *et al.* Cohesins and condensins orchestrate the 4D dynamics of yeast chromosomes during the cell cycle. *EMBO J* **36**, 2684–2697 (2017).

26. Duan, Z. *et al.* A three-dimensional model of the yeast genome. *Nature* **465**, 363–367 (2010).

27. Wong, H. A predictive computational model of the dynamic 3D interphase yeast nucleus. *Curr Biol* **22**, 1881–1890 (2012).

28. Dauban, L. *et al.* Regulation of Cohesin-Mediated Chromosome Folding by Eco1 and Other Partners. *Mol Cell* **77**, 1279-1293.e4 (2020).

29. Costantino, L., Hsieh, T.-H. S., Lamothe, R., Darzacq, X. & Koshland, D. Cohesin residency determines chromatin loop patterns. *Elife* **9**, e59889 (2020).

30. Lengronne, A. *et al.* Cohesin relocation from sites of chromosomal loading to places of convergent transcription. *Nature* **430**, 573–578 (2004).

31. Glynn, E. F. Genome-wide mapping of the cohesin complex in the yeast Saccharomyces cerevisiae. *PLoS Biol* **2, E259**, (2004).

32. Rao, S. S. P. A 3D map of the human genome at kilobase resolution reveals principles of chromatin looping. *Cell* **159**, 1665–1680 (2014).

33. Goloborodko, A., Imakaev, M. V., Marko, J. F. & Mirny, L. Compaction and segregation of sister chromatids via active loop extrusion. *Elife* **5**, e14864 (2016).

34. Haarhuis, J. H. I. *et al.* The Cohesin Release Factor WAPL Restricts Chromatin Loop Extension. *Cell* **169**, 693-707.e14 (2017).

35. Spracklin, G. *et al.* Diverse silent chromatin states modulate genome compartmentalization and loop extrusion barriers. *Nat Struct Mol Biol* **30**, 38–51 (2023).

510 36. Nora, E. P. Targeted Degradation of CTCF Decouples Local Insulation of Chromosome
511 Domains from Genomic Compartmentalization. *Cell* **169**, 930-944 22 (2017).
512 37. Naumova, N. Organization of the mitotic chromosome. *Science* **342**, 948–953 (2013).
513 38. Struhl, K. & Segal, E. Determinants of nucleosome positioning. *Nat Struct Mol Biol* **20**, 267–
514 273 (2013).
515 39. Gvozdenov, Z., Barcutean, Z. & Struhl, K. Functional analysis of a random-sequence
516 chromosome reveals a high level and the molecular nature of transcriptional noise in yeast
517 cells. *Molecular Cell* **0**, (2023).
518 40. Luthra, I. *et al.* Biochemical activity is the default DNA state in eukaryotes.
519 2022.12.16.520785 Preprint at https://doi.org/10.1101/2022.12.16.520785 (2022).
520 41. Camellato, P., Brosh, R., Maurano, M. & Boeke, J. Genomic analysis of a synthetic reversed
521 sequence reveals default chromatin states in yeast and mammalian cells. bioRxiv. (2022).
522 42. Ocampo-Hafalla, M., Muñoz, S., Samora, C. P. & Uhlmann, F. Evidence for cohesin sliding
523 along budding yeast chromosomes. *Open Biol* **6**, 150178 (2016).
524 43. de Boer, C. G. *et al.* Deciphering eukaryotic gene-regulatory logic with 100 million random
525 promoters. *Nat Biotechnol* **38**, 56–65 (2020).
526 44. Vaishnav, E. D. The evolution, evolvability and engineering of gene regulatory DNA. *Nature*
527 **603**, 455–463 (2022).
528 45. Koster, C. C., Postma, E. D., Knibbe, E., Cleij, C. & Daran-Lapujade, P. Synthetic Genomics
529 From a Yeast Perspective. *Front. Bioeng. Biotechnol.* **10**, 869486 (2022).
530 46. Schindler, D. *et al.* Design, Construction, and Functional Characterization of a tRNA
531 Neochromosome in Yeast. 2022.10.03.510608 Preprint at
532 https://doi.org/10.1101/2022.10.03.510608 (2022).
533 47. Ginno, P. A., Lott, P. L., Christensen, H. C., Korf, I. & Chédin, F. R-loop formation is a
534 distinctive characteristic of unmethylated human CpG island promoters. *Mol Cell* **45**, 814–
535 825 (2012).

536 48. Lobry, J. R. Asymmetric substitution patterns in the two DNA strands of bacteria. *Mol Biol*
537 *Evol* **13**, 660–665 (1996).
538 49. Schulz, D. Transcriptome Surveillance by Selective Termination of Noncoding RNA
539 Synthesis. *Cell* **155**, 1075–1087 (2013).
540 50. Bastie, N. *et al.* Sister chromatid cohesion halts DNA loop expansion. 2023.07.31.551217
541 Preprint at https://doi.org/10.1101/2023.07.31.551217 (2023).
542 51. Banigan, E. J. *et al.* Transcription shapes 3D chromatin organization by interacting with loop
543 extrusion. *Proceedings of the National Academy of Sciences* **120**, e2210480120 (2023).
544 52. Dequeker, B. J. H. *et al.* MCM complexes are barriers that restrict cohesin-mediated loop
545 extrusion. *Nature* **606**, 197–203 (2022).
546 53. Hergeth, S. P. & Schneider, R. The H1 linker histones: multifunctional proteins beyond the
547 nucleosomal core particle. *EMBO Rep* **16**, 1439–1453 (2015).
548

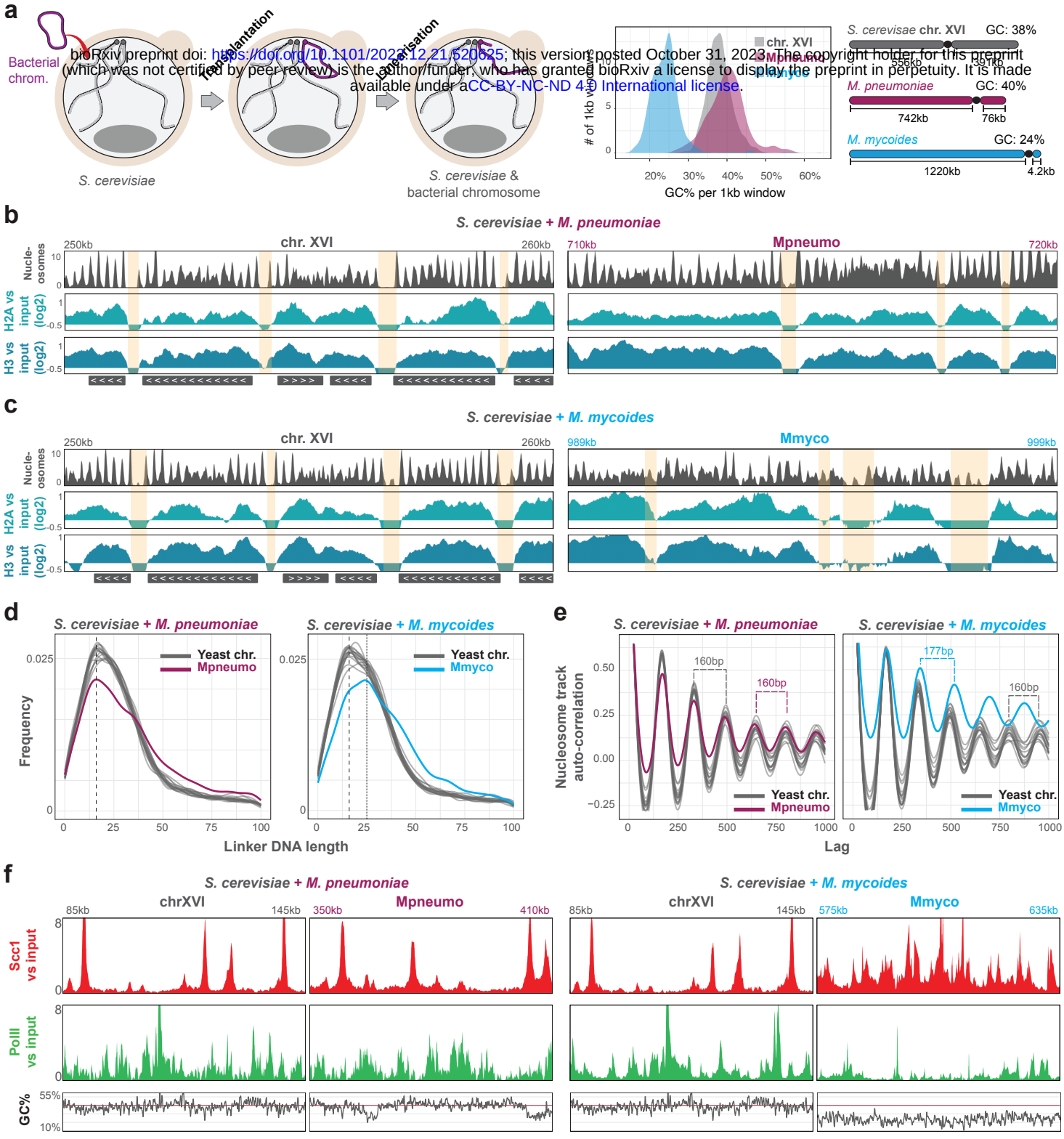

Fig. 1

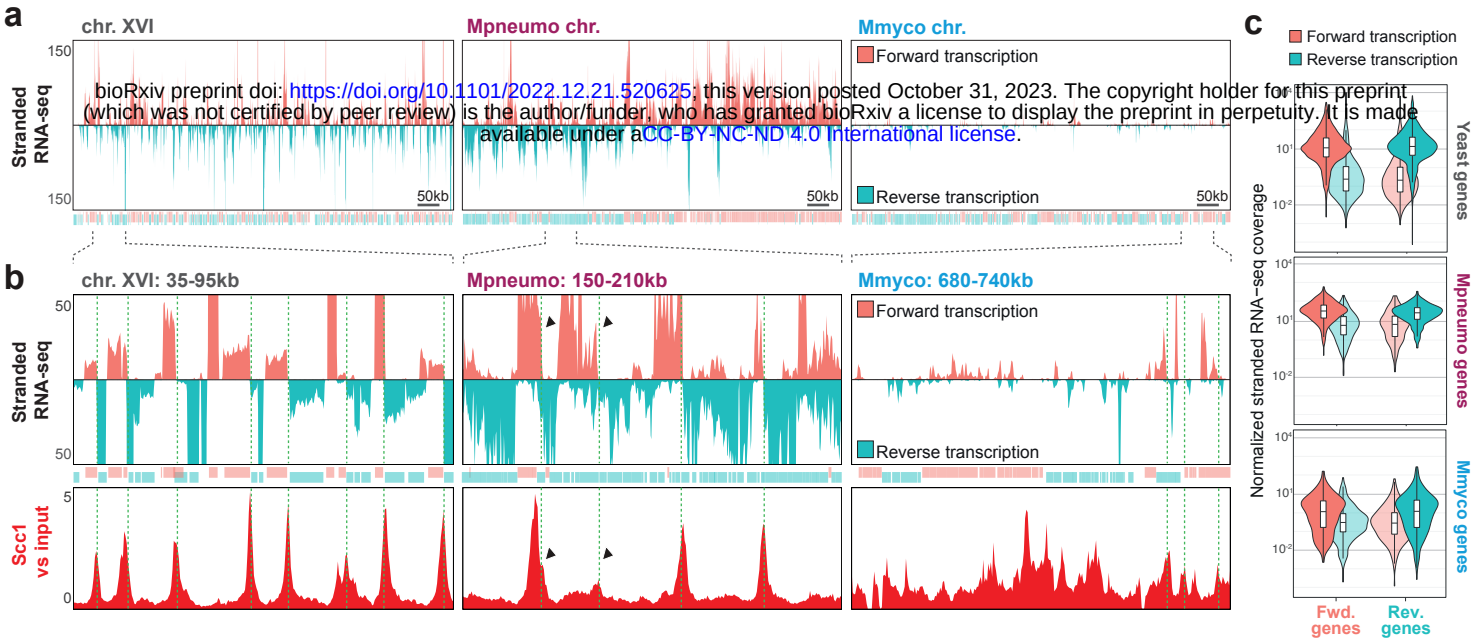

Fig. 2

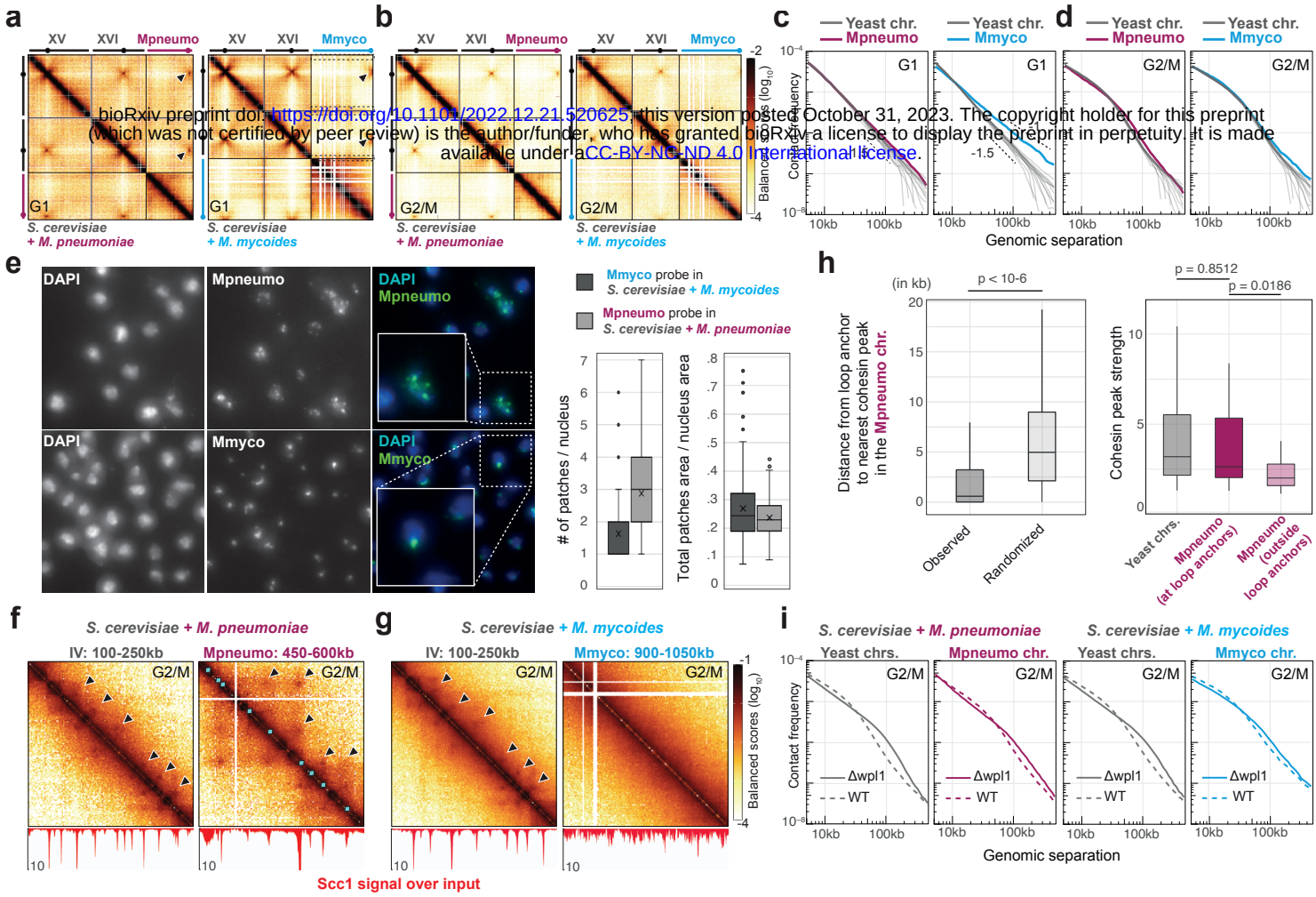

Fig. 3

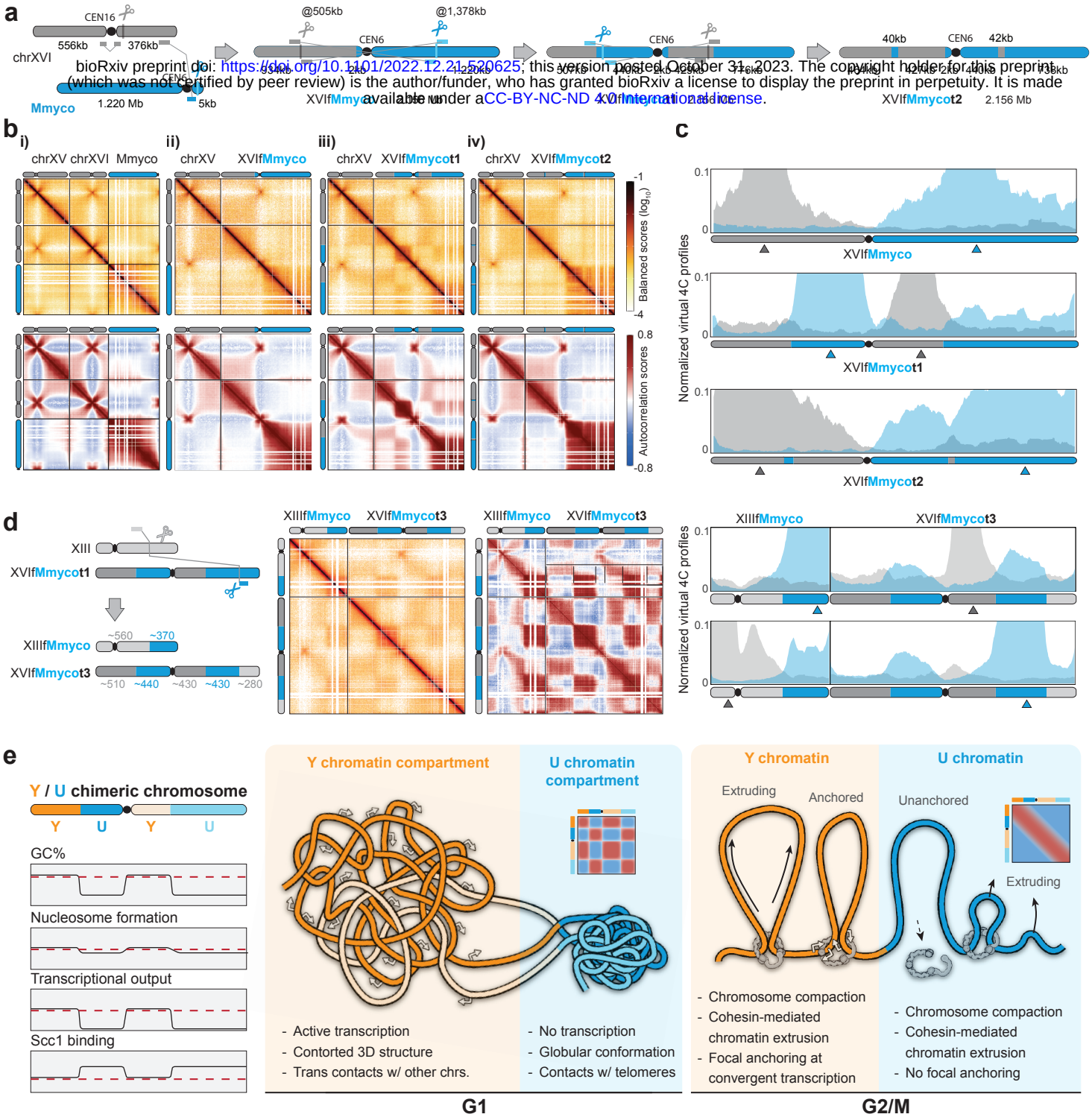

Fig. 4